

# Theoretical utmost performance of (100) mid-wave HgCdTe photodetectors

P. Martyniuk\*, W. Gawron, P. Madejczyk, M. Kopytko, K. Grodecki, E. Gomułka

Institute of Applied Physics, Military University of Technology, 2 Kaliskiego Str.,  
00-908 Warsaw, Poland (✉ [piotr.martyniuk@wat.edu.pl](mailto:piotr.martyniuk@wat.edu.pl), +48 22 6839673)

**Abstract** – Except Auger 7, *p*-type HgCdTe is mostly limited by technology dependent Shockley-Read-Hall generation-recombination processes. One of the ways to reduce the trap density is a growth of the (100) HgCdTe on GaAs substrates. That orientation allows reaching lower carrier concentration  $\sim 5 \times 10^{14} \text{ cm}^{-3}$  in comparison to the commonly used (111) orientation  $\sim 5 \times 10^{15} \text{ cm}^{-3}$  in mid-wave infrared range. In addition Shockley-Read-Hall traps density could be reduced to the level of  $\sim 4.4 \times 10^8 \text{ cm}^{-3}$ . The theoretical simulations related to the utmost performance of the (100) HgCdTe Auger suppressed structures are presented. Dark current is reported to be reduced by more than one order of magnitude within the range  $\sim 6 \times 10^{-2} - 3 \times 10^{-3} \text{ A/cm}^2$ . Detectivity increases within range  $\sim 3 - 12 \times 10^{11} \text{ cmHz}^{1/2}/\text{W}$  (wavelength  $\sim 5 \mu\text{m}$ ) at temperature 200 K and voltage 200 mV.

## I. INTRODUCTION

Without optical immersion (GaAs substrate - converted into immersion lens) mid-wave infrared radiation (MWIR) HgCdTe photovoltaic detectors are reported to exhibit nearly background limited performance (BLIP) [1,2]. As substrates epitaxially GaAs wafers of different orientation and interdiffused multilayer process (IMP) are used in HgCdTe growth [3].

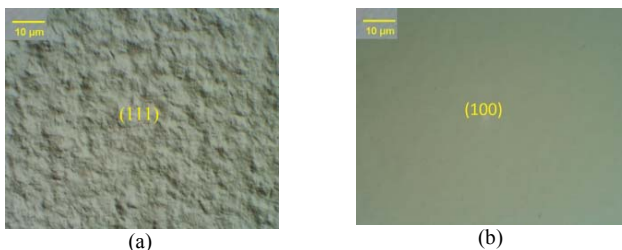


Fig. 1. Surface morphology of (111) - (a) and (100) - (b) HgCdTe layers.

Epitaxially (100) GaAs substrates exhibit  $\sim 14.6\%$  lattice mismatch with CdTe buffer layer. That mismatch allows to grow both (100) and (111) orientations. In addition, the monolithic optical immersion results in significant improvement in detectivity by  $\sim n^2$  where  $n$  stands for GaAs refractive index [4].

Figure 1 (a) and (b) shows the difference in surface morphology between two analyzed HgCdTe orientations. As it is presented in Fig. 1, the (100) HgCdTe orientation tends to be almost mirror-smooth. In addition (100) HgCdTe epilayers have higher As doping efficiency and is an attractive plane for fabrication of the abrupt heterojunctions. Even though the (100) surface morphology is superior to the (111), the (100) orientation is characterized by pyramid-shaped macrodefects known as *hillocks* shown in both surface and cleavage

presented in Fig. 2 (a) and (b). Epilayers with *hillocks* are practically useless for device fabrication. According to literature, only Selex Galileo reported on suppression of *hillocks* density below  $5 \text{ cm}^{-2}$  in the (100) HgCdTe grown on GaAs [5, 6]. Therefore, most of the reported devices are based on (111) layers [7]. In this paper we present the theoretical simulations related to the utmost performance of the (100) HgCdTe MWIR, multi-layer structures grown on GaAs substrates.

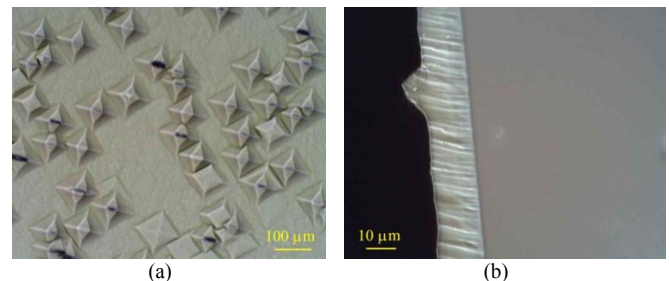


Fig. 2. Hillocks on (100) HgCdTe layers: surface (a); cleavage (b).

High-quality MWIR detectors require HgCdTe layers with low dislocation density. The (100) HgCdTe orientation allows to reduce *p*-type doping to the level of  $\sim 5 \times 10^{14} \text{ cm}^{-3}$  in analyzed MWIR range. In addition Shockley-Read-Hall (SRH) traps density could be reduced to the level of  $\sim 4.4 \times 10^8 \text{ cm}^{-3}$  resulting in suppression of the dark current ( $J_{\text{DARK}} \sim 6 \times 10^{-2} - 3 \times 10^{-3} \text{ A/cm}^2$ ). Detectivity ( $D^*$ ) increases within range  $\sim 3 - 12 \times 10^{11} \text{ cmHz}^{1/2}/\text{W}$  for wavelength,  $\lambda \sim 5 \mu\text{m}$  at temperature 200 K and voltage 200 mV.

The 77 K carrier concentration for the Cd composition,  $x_{\text{Cd}}$  for two analyzed orientations (111) and (100) is presented in Fig. 3. The assumed in calculations carrier concentrations are fully confirmed within the range composition corresponding to the MWIR range reached in MOCVD machine.

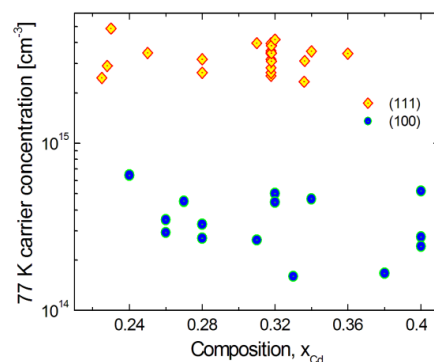
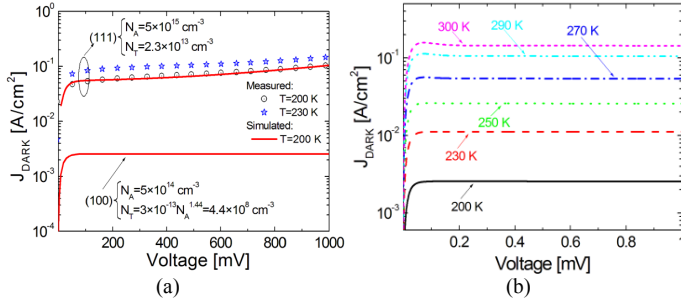


Fig. 3. Measured 77 K carrier concentration for analyzed (100) and (111) orientations.

## II. SIMULATION PROCEDURE AND RESULTS

The detailed description of the MWIR detector and simulation procedure is described in detail in Ref. 8. The doping in active layer and trap density was reduced to correspond to the level presented in Fig. 3. Proper doping grading were introduced to prevent form discontinuities in energy band profiles between absorber ( $\pi$ )-N<sup>+</sup> contact and absorber ( $\pi$ )-P<sup>+</sup> heterojunctions.

Measured and simulated  $J_{DARK}$  versus voltage for both (111) and (100) orientations are presented in Fig. 4. Active layer doping reduction to the level presented in Fig. 3 suppresses both band-to-band and trap-assisted tunneling mechanisms. Slight Auger suppression is seen above 290 K [Fig. 4 (b)].



**Fig. 4.** Theoretically simulated and measured dark current density versus voltage for (111) orientation grown on GaAs - absorber doping,  $N_A = 5 \times 10^{15} \text{ cm}^{-3}$ ; trap density,  $N_T = 2.3 \times 10^{13} \text{ cm}^{-3}$  and (100) orientation  $N_A = 5 \times 10^{14} \text{ cm}^{-3}$ ; trap density,  $N_T = 4.4 \times 10^8 \text{ cm}^{-3}$  (a).  $J_{DARK}$  versus voltage for selected temperatures,  $T = 200\text{--}300 \text{ K}$  (b).

The noise current was simulated using the following expression to include both the thermal Johnson-Nyquist noise and electrical shot noise contributions:

$$i_n(V) = \sqrt{(4k_B T / RA + 2qJ_{DARK})A}, \quad (1)$$

where  $A$  is the area of the detector ( $100 \times 100 \mu\text{m}^2$ ),  $RA$  is the dynamic resistance area product,  $J_{DARK}$  is the dark current density, and  $k_B$  is the Boltzmann constant. Detectivity is defined by the following expressions to include the effect of the GaAs immersion lens ( $n$  - GaAs refractive index):

$$D^* = \frac{R_i}{i_n(V)} n^2 \sqrt{A}. \quad (2)$$

The structure with (100) orientation and integrated GaAs immersion lens reaches  $\sim 10^{12} \text{ cmHz}^{1/2}/\text{W}$  ( $T = 200 \text{ K}$ ) being one order magnitude higher than BLIP detectivity  $\sim 10^{11} \text{ cmHz}^{1/2}/\text{W}$  at  $\lambda \sim 5 \mu\text{m}$  and reported previously for structures with (111) orientation presented in Fig. 5.

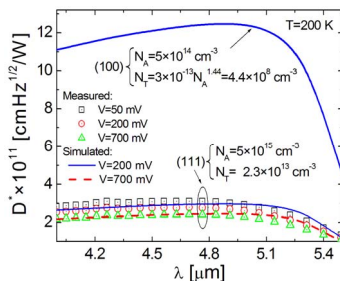


**Fig. 5.** Theoretically simulated and measured detectivity versus wavelength for (111) orientation grown on GaAs - absorber doping,  $N_A = 5 \times 10^{15} \text{ cm}^{-3}$ ; trap density,  $N_T = 2.3 \times 10^{13} \text{ cm}^{-3}$  and (100) orientation  $N_A = 5 \times 10^{14} \text{ cm}^{-3}$ ; trap density,  $N_T = 4.4 \times 10^8 \text{ cm}^{-3}$ .

Time response was simulated versus voltage [Fig. 6 (a)] and temperature for  $V = 250 \text{ mV}$  [Fig. 6 (b)]. For the (100) orientation time response,  $\tau_s$  reaches  $\sim 4100\text{--}1100 \text{ ps}$  for voltage range  $50\text{--}400 \text{ mV}$  being nearly two times lower in comparison to the (111) orientation for  $V = 400 \text{ mV}$ . Series resistance was assumed to be within range  $190\text{--}510 \Omega$ .

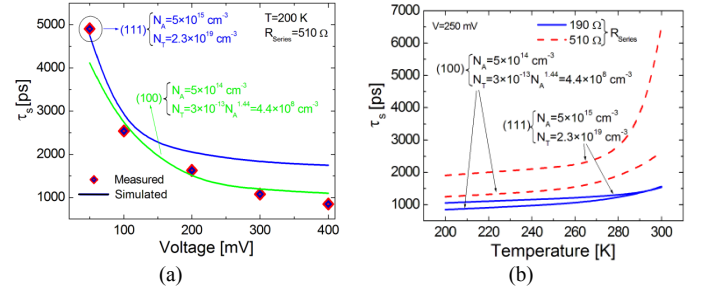


**Fig. 6.** Measured and theoretically simulated time response versus voltage (a) and temperature for (111) orientation grown on GaAs - absorber doping,  $N_A = 5 \times 10^{15} \text{ cm}^{-3}$ ; trap density,  $N_T = 2.3 \times 10^{13} \text{ cm}^{-3}$  and (100) orientation  $N_A = 5 \times 10^{14} \text{ cm}^{-3}$ ; trap density,  $N_T = 4.4 \times 10^8 \text{ cm}^{-3}$ .  $R_{Series} = 190$  and  $510 \Omega$ .

## III. CONCLUSIONS

Theoretical utmost performance of the (100) HgCdTe grown on GaAs substrate MWIR photodetector was presented. It is predicted that trap density could be reduced to  $\sim 4.4 \times 10^8 \text{ cm}^{-3}$  assuming active layer doping  $\sim 5 \times 10^{14} \text{ cm}^{-3}$ . Those active layers parameters results in suppression of the dark current  $\sim 6 \times 10^{-2}\text{--}3 \times 10^{-3} \text{ A/cm}^2$ . Detectivity increases within range  $\sim 3\text{--}12 \times 10^{11} \text{ cmHz}^{1/2}/\text{W}$  at temperature  $200 \text{ K}$  and voltage  $200 \text{ mV}$ . Suppression of the trap density to the level of  $\sim 4.4 \times 10^8 \text{ cm}^{-3}$  allows reaching better performance in frequency response  $\sim 859 \text{ ps}$  corresponding to  $200 \text{ K}$  and  $V = 200 \text{ mV}$ ,  $R_{Series} = 190 \text{ K}$ .

## ACKNOWLEDGMENT

This paper has been completed with the financial support of the Polish National Science Centre, Projects: 2013/08/A/ST5/00773 and 2013/08/M/ST7/00913.

## REFERENCES

- [1] J. Piotrowski, A. Rogalski, High-operating temperature infrared photodetectors, SPIE Press, Bellingham, 2007.
- [2] A. Rogalski, Infrared detectors, CRC Press, Boca Raton, 2011.
- [3] J. C. Irvine, "Recent development in MOCVD of Hg<sub>1-x</sub>Cd<sub>x</sub>Te," Proc. SPIE 1735, 92–99 (1992).
- [4] J. Piotrowski, A. Rogalski, "Uncooled long wavelength infrared photon detectors," Infrared Physics & Technol. 46, 115–131 (2004).
- [5] C. D. Maxey, M. U. Ahmed, P. Capper, C. L. Jones, N. T. Gordon, M. White, "Investigation of parameters to obtain reduced Shockley-Read traps and near radiatively limited lifetimes in MOVPE-grown MCT", J. Mater. Sci. Mater. Electron. 11, 565–568 (2000).
- [6] C. D. Maxey, J. C. Fitzmaurice, H. W. Lau, L. G. Hipwood, C. S. Shaw, C. L. Jones, P. Capper, "Current status of large-area MOVPE growth of HgCdTe device heterostructures for infrared focal plane arrays", J. Electron. Mater. 35, 1275–1282 (2006).
- [7] P. Madejczyk, W. Gawron, P. Martyniuk, A. Kęłowski, A. Piotrowski, J. Pawluczyk, W. Pusz, A. Kowalewski, J. Piotrowski, A. Rogalski, "MOCVD grown HgCdTe device structure for ambient temperature LWIR detectors", Semicond. Sci. Technol. 28, 10, 105017-1–7 (2013).
- [8] P. Martyniuk, W. Gawron, A. Rogalski, "Modeling of HOT (111) HgCdTe MWIR detector for fast response operation", Opt Quant Electron 46, 10, 1303–1312 (2014).